Epigenetic Silencing of CHOP Expression by the Histone Methyltransferase EHMT1 Regulates Apoptosis in Colorectal Cancer Cells

Kwangho Kim[1,3,4], Tae Young Ryu[1,4], Jinkwon Lee[1,2], Mi-Young Son[1,2], Dae-Soo Kim[1,2], Sang Kyum Kim[3,*], and Hyun-Soo Cho[1,2,*]

[1]Korea Research Institute of Bioscience and Biotechnology, Daejeon 34141, Korea, [2]Department of Functional Genomics, Korea University of Science and Technology, Daejeon 34113, Korea, [3]College of Pharmacy, Chungnam National University, Daejeon 34134, Korea, [4]These authors contributed equally to this work.
*Correspondence: chohs@kribb.re.kr (HSC); sangkim@cnu.ac.kr (SKK)
https://doi.org/10.14348/molcells.2022.0014
www.molcells.org

Colorectal cancer (CRC) has a high mortality rate among cancers worldwide. To reduce this mortality rate, chemotherapy (5-fluorouracil, oxaliplatin, and irinotecan) or targeted therapy (bevacizumab, cetuximab, and panitumumab) has been used to treat CRC. However, due to various side effects and poor responses to CRC treatment, novel therapeutic targets for drug development are needed. In this study, we identified the overexpression of EHMT1 in CRC using RNA sequencing (RNA-seq) data derived from TCGA, and we observed that knocking down EHMT1 expression suppressed cell growth by inducing cell apoptosis in CRC cell lines. In Gene Ontology (GO) term analysis using RNA-seq data, apoptosis-related terms were enriched after EHMT1 knockdown. Moreover, we identified the CHOP gene as a direct target of EHMT1 using a ChIP (chromatin immunoprecipitation) assay with an anti-histone 3 lysine 9 dimethylation (H3K9me2) antibody. Finally, after cotransfection with siEHMT1 and siCHOP, we again confirmed that CHOP-mediated cell apoptosis was induced by EHMT1 knockdown. Our findings reveal that EHMT1 plays a key role in regulating CRC cell apoptosis, suggesting that EHMT1 may be a therapeutic target for the development of cancer inhibitors.

Keywords: apoptosis, C/EBP homologous protein, colorectal cancer, euchromatic histone-lysine N-methyltransferase 1

INTRODUCTION

Colorectal cancer (CRC) is the third most common cause of death worldwide and ranks second among all cancers in mortality (Sung et al., 2021). The most common way to treat CRC is surgery. However, cancer cells are difficult to completely remove, and because the remaining cancer cells can metastasize to other parts of the body, chemotherapy has been recognized as an important method for CRC treatment (Kuipers et al., 2015). Currently, chemotherapy using 5-fluorouracil, capecitabine, irinotecan, and oxaliplatin is available for CRC patients. There are also targeted therapies, such as bevacizumab (inhibits blood vessel formation), cetuximab, panitumumab (targets cancer cells by modulating EGFR), and encorafenib (targets cancer cells by altering the BRAF gene) (Koopman et al., 2007; Xie et al., 2020). However, as existing anticancer drugs have limitations in the form of various side effects, low response rates, drug resistance, and low tumor-specific selectivity, novel therapeutic targets for CRC treatment are needed.

Recently, enzymes modifying epigenetic factors such as

DNA methylation and histone marks have attracted attention as therapeutic targets for the suppression of the growth and metastasis of CRC (Baretti and Azad, 2018; Jung et al., 2020). Among them, euchromatic histone-lysine N-methyltransferase 1 (EHMT1), also known as GLP (G9a-like protein), is a histone methyltransferase that mainly induces histone H3 lysine 9 (H3K9) monomethylation and dimethylation. EHMT1 and G9a form a heteromeric complex and drive transcriptional silencing through euchromatin methylation at H3K9. EHMT1 negatively regulates the NF-kB and type I interferon induction pathways (Ea et al., 2012) and forms a transcriptional complex with PR domain-containing 16 (PRDM16), thereby regulating brown adipose cell fate, thermogenesis, and glucose homeostasis (Ohno et al., 2013). In addition, EHMT1 regulates various physiological functions, such as fetal hemoglobin, cardiac hypertrophy, and intellectual disability (Kleefstra et al., 2012; Renneville et al., 2015; Thienpont et al., 2017). Furthermore, several studies have indicated that overexpression of EHMT1 is observed in several types of cancer, including breast cancer, gastric cancer, and esophageal squamous cell cancer, suggesting that EHMT1 is related to tumor development and metastasis progression (Cebrian et al., 2006; Guan et al., 2014; Yang et al., 2018). In a previous study, we also overexpressed EHMT1 and confirmed that EHMT1 directly regulates CDKN1A in lung cancer, causing cell cycle arrest and inducing apoptosis (Lee et al., 2021). However, in CRC, the function of EHMT1 is not fully understood.

Therefore, in this study, we identified overexpression of EHMT1 with CRC RNA sequencing (RNA-seq) data derived from TCGA and found that cell apoptosis was induced by EHMT1 knockdown via direct epigenetic upregulation of C/EBP homologous protein (CHOP) expression. Thus, we propose that EHMT1 is a potential therapeutic target for the development of anticancer drugs for CRC treatment.

MATERIALS AND METHODS

Cell culture and reagents
The human CRC cell lines HCT116 and HT-29 were purchased from the Korean Cell Line Bank and cultured in RPMI-1640 medium supplemented with 10% fetal bovine serum (FBS) and 1% penicillin/streptomycin in a humidified atmosphere with 5% CO_2 at 37°C.

siRNA transfection
For siRNA transfection, HCT116 and HT-29 cells were seeded in plates and incubated for 24 h. The targeting and control siRNAs (Bioneer, Korea) were transfected into cancer cell lines at 100 nM using RNAiMax (Invitrogen, USA) for 48 h. The sequences of the siRNAs used were as follows: siCont (5'-AUGAACGUGAAUUGCUCAATT-3', 5'-UUGAGCAAUUCAC-GUUC AUTT-3'), siEHMT1 (5'-CUCAGAACCAGUGCUACAU T-3', 5'-AUGUAGCACUGGU UCUGAGTT-3'), and siCHOP (5'-CUGACUACCCUCU CACUAG TT-3', 5'-CUAGUGAGA GGGUAGUCAGTT-3').

Cell viability assay
Cell counting kit-8 (CCK-8) (E-CK-A361; Elabscience, USA) was used to conduct cell viability assays. HCT116 and HT-29 cells were seeded in 6-well plates at 2×10^5 cells/well and incubated for 24 h. After siRNA transfection for 48 h, CCK8 solution and RPMI-1640 medium with 10% FBS were added to each well and incubated with 5% CO_2 at 37°C for 2 min or 5 min. The absorbance was assessed using a microplate reader at 450 nm. For crystal violet staining, the cells were fixed with methanol for 5 min and stained with 0.1% crystal violet after siRNA transfection for 48 h.

FACS analysis
After siRNA transfection for 48 h, the cells were collected and incubated with the Muse Annexin V and Dead Cell Assay kit (MCH100105; Luminex, USA) for 20 min at room temperature. For analysis using the Muse™ Caspase-3/7 Kit (MCH100108; Luminex), the cells were incubated with caspase 3/7 reagent (Merck, Germany) for 30 min in a humidified atmosphere with 5% CO_2 at 37°C. After incubation, the cells were incubated with Caspase 7-AAD (Merck) for 5 min at room temperature. After incubation, ~5×10^4 cells were analyzed using a Muse Cell analyzer (Merck). The FACS results were analyzed using Muse 1.5 Analysis software (Merck).

Quantitative real-time polymerase chain reaction (qRT-PCR)
Total RNA was isolated from the indicated cell lines using a Qiagen RNeasy Mini Kit according to the manufacturer's instructions. RNA aliquots of 1 μg were then reverse transcribed using PrimeScript RT Master Mix (RR036A; Takara, Japan) according to standard protocols. For qRT-PCR, the reactions were performed using the AriaMx Real-Time PCR kit (Agilent Technologies, USA) following the manufacturer's instructions. qRT-PCR was performed on cDNA samples using Brilliant III Ultra-Fast SYBR® Green QPCR Master Mix (Agilent Technologies), and the signal was detected by an AriaMx Real-time PCR System (Agilent Technologies). The fluorescence threshold value was calculated using Agilent Aria 1.6 software. The PCR primers used were as follows: EHMT1 (forward, 5'-CAGGACTTCCAAGGAGAGCA-3' and reverse, 5'-ACTCAGGT-CAGACTCGT CAC-3'), CHOP (forward, 5'-GGAAACAGAGT-GGTCAT TCCC-3' and reverse, 5'-CTGCTTGA GCCGTTCAT-TCTC-3'), GRP78 (forward, 5'-CA TCACGCCGTCCTATGTCG-3' and reverse, 5'-CGTCAAAGACCGTGTTCTCG-3'), ATF4 (forward, 5'-ATGACCGAAATGAGCTT CCTG-3' and reverse, 5'-GCTGGAGAA CCCATGAGGT-3'), and ACTB (forward, 5'-ACT CTTCCAGCCTTCCTTCC-3' and reverse, 5'-CAATGCCAG-GGTACATGGTG-3').

Western blotting analysis
The cells were washed once with phosphate-buffered saline (PBS) and then lysed in cold lysis buffer (50 mM TrisHCl, pH 7.4, 150 mM NaCl, 1% Triton X-100, 0.1% SDS, 1 mM EDTA, 1 mM Na_3VO_4, 1 mM NaF, and 1× protease inhibitor cocktail). Cell lysates were centrifuged at 14,000 × g for 15 min at 4°C and then boiled in 5× sample buffer following protein determination (BSA, #23208; Thermo Fisher Scientific, USA). The protein samples were subjected to western blotting analysis. For western blotting analysis, nitrocellulose

membranes (#1620145; Bio-Rad, USA), blocking reagent (5% skim milk, 1 h, room temperature), and precasting gels (#456-1095; Bio-Rad) were used with the indicated antibodies at a 1:1,000 dilution ratio. The samples were stained with rabbit anti-EHMT1 antibody (A301-642A; Bethyl Laboratories, USA), mouse anti-CHOP antibody (#2895; Cell Signaling Technology, USA), rabbit anti-PARP antibody (#9542; Cell Signaling Technology) and mouse anti-ACTB antibody (SC-47778; Santa Cruz Biotechnology, USA) at 4°C (overnight). Secondary antibodies (rabbit: SC-2357, mouse: SC-516102; Santa Cruz Biotechnology) were incubated at room temperature for 1 h, and ECL solution (#170-5060; Bio-Rad) was used for visualization.

Chromatin immunoprecipitation (ChIP) assay
ChIP was performed with a Simple ChIP® Plus Sonication Chromatin IP Kit (#56383S; Cell Signaling Technology) following the manufacturers' instructions. HCT116 cells transfected with siCont and siEHMT1 for 48 h were crosslinked with 1% formaldehyde (Sigma-Aldrich, USA) for 10 min at room temperature and quenched with 1× glycine for 5 min at room temperature. Then, the cells were washed with cold 1× PBS (containing 1× Protease Inhibitor Cocktail) and lysed in 1× cell lysis buffer (containing 1× Protease Inhibitor Cocktail). Next, after nuclear extraction, the chromatin solution was sonicated using a Bioruptor® Pico sonication device (B01060010; Diagenode, USA) with 15 cycles of 30 s ON and 30 s OFF to obtain 200-1,000 bp chromatin fragments. Sheared chromatin (approximately 5-10 μg) was incubated with 2 μg of ChIP-grade anti-H3K9me2 antibody (ab1220; Abcam, UK) at 4°C (overnight). After overnight incubation, complexes with 30 μl of ChIP-Grade Protein G Magnetic Beads were incubated for 2 h at 4°C. Then, the complexes were washed for each step and incubated with ChIP elution buffer for 30 min at 65°C and then incubated with proteinase K for 2 h at 65°C. After DNA purification using spin columns, the samples were analyzed by qRT-PCR using CHOP primers. The primers were as follows: CHOP (P1) (forward, 5'-TCCACTGGGCAAAATA-CATGAC-3' and reverse, 5'-CAAAAAAACGGGGGTGGTC-3'), CHOP (P2) (forward, 5'-CCACCCCCGTTTTTTTG TTT-3' and reverse, 5'-ATT AGCCGGGT GTGGTGA-3'), CHOP (P3) (forward, 5'-ACCACACCCGGCTAATTT-3' and reverse, 5'-CAT CCACTGGGATTGTCGAC-3')'.

RNA-seq and analysis
Using a TruSeq RNA Sample Preparation Kit V2, purification and library construction were conducted with total RNA, and Illumina HiSeq 2500 machines (Illumina, USA) were used for sequencing with a read length of 2 × 100 bases. FastQC v.0.11.4 was used to assess the quality of the paired-end reads. Cutadapt v.1.15 and Sickle v. 1.33 were used to filter low-quality reads and adaptors. Cufflinks version 2.2.1 was used to calculate fragments per kilobase of transcripts per million mapped reads (FPKM) values. Cuffdiff was used to select differentially expressed genes (DEGs) (fold change > 2). All GO analyses were performed using DAVID ver. 6.8 and ClueGO ver. 2.5.5 in Cytoscape ver. 3.7.1.

Statistical analysis
The results are expressed as the mean ± SD of three independent experiments. Student's t-test was performed using GraphPad Prism 5.0 (GraphPad Software, USA). The cutoff for significance was $P < 0.05$.

RESULTS

EHMT1 is overexpressed in CRC
To assess the expression level of EHMT1 in CRC, we used RNA-seq data from CRC samples and normal samples derived from TCGA and found overexpression of EHMT1 in CRC samples compared to normal samples (Fig. 1A). Using EHMT1-specific small interfering RNA (siRNA) and a negative control (siCont), we evaluated the biological function of EHMT1 in the HCT116 and HT-29 cell lines. After treatment with siEHMT1 and siCont, the expression of EHMT1 was significantly decreased (Fig. 1B), and we found inhibition of cell growth with siEHMT1 compared to siCont treatment via CV staining and CCK-8 assay in both cell lines (Figs. 1C and 1D). Thus, we clearly found that EHMT1 could be related to CRC cell proliferation. Next, to evaluate how EHMT1 knockdown induces cell growth suppression, we performed western blotting and fluorescence-activated cell sorting (FACS) analyses. In western blotting analysis, cleaved PARP was found to be increased by knockdown of EHMT1 compared to treatment with siCont in HCT116 and HT-29 cells (Fig. 1E). Moreover, the FACS analysis determining annexin V staining and caspase-3/7 activity showed that the total apoptotic cell population (early and late) was significantly increased after EHMT1 knockdown compared to siCont treatment, and caspase 3/7 activity was also upregulated by EHMT1 knockdown in HCT116 and HT-29 cells (Figs. 1F and 1G). Taken together, these results indicate that downregulation of EHMT1 inhibits cell growth via cell apoptosis.

CHOP is a direct target of EHMT1 in CRC
To determine the function of EHMT1 in CRC, we performed RNA-seq analysis after treatment of HCT116 cells with siCont and siEHMT1. A total of 930 dysregulated genes were identified (473 upregulated genes and 457 downregulated genes in siEHMT1-treated cells) (cutoff, 2.0-fold; $P > 0.05$), and we performed Gene Ontology (GO) analysis via the Database for Annotation, Visualization and Integrated Discovery (DAVID) and the CluGO plug in Cytoscape (ver. 3.7.1). Fig. 2A shows that apoptosis-related terms were enriched by knocking down EHMT1 expression in HCT116 cells, suggesting that EHMT1 is a potential regulator of CRC cell apoptosis (Figs. 2A and 2B).

EHMT1 is a histone methyltransferase that induces H3K9 dimethylation (H3K9me2) to construct a heterochromatin structure for suppression of gene expression at the transcriptional level. Thus, to identify direct target genes of EHMT1, we focused on the upregulated genes in the RNA-seq results and ultimately selected the CHOP gene among six genes (CHOP, polo-like kinase 3 [PLK3], DNA damage regulated autophagy modulator 1 [DRAM1], estrogen receptor binding site-associated antigen 9 [EBAG9], S100 calcium binding protein A14 [S100A14], and galectin 1 [LGALS1]), which
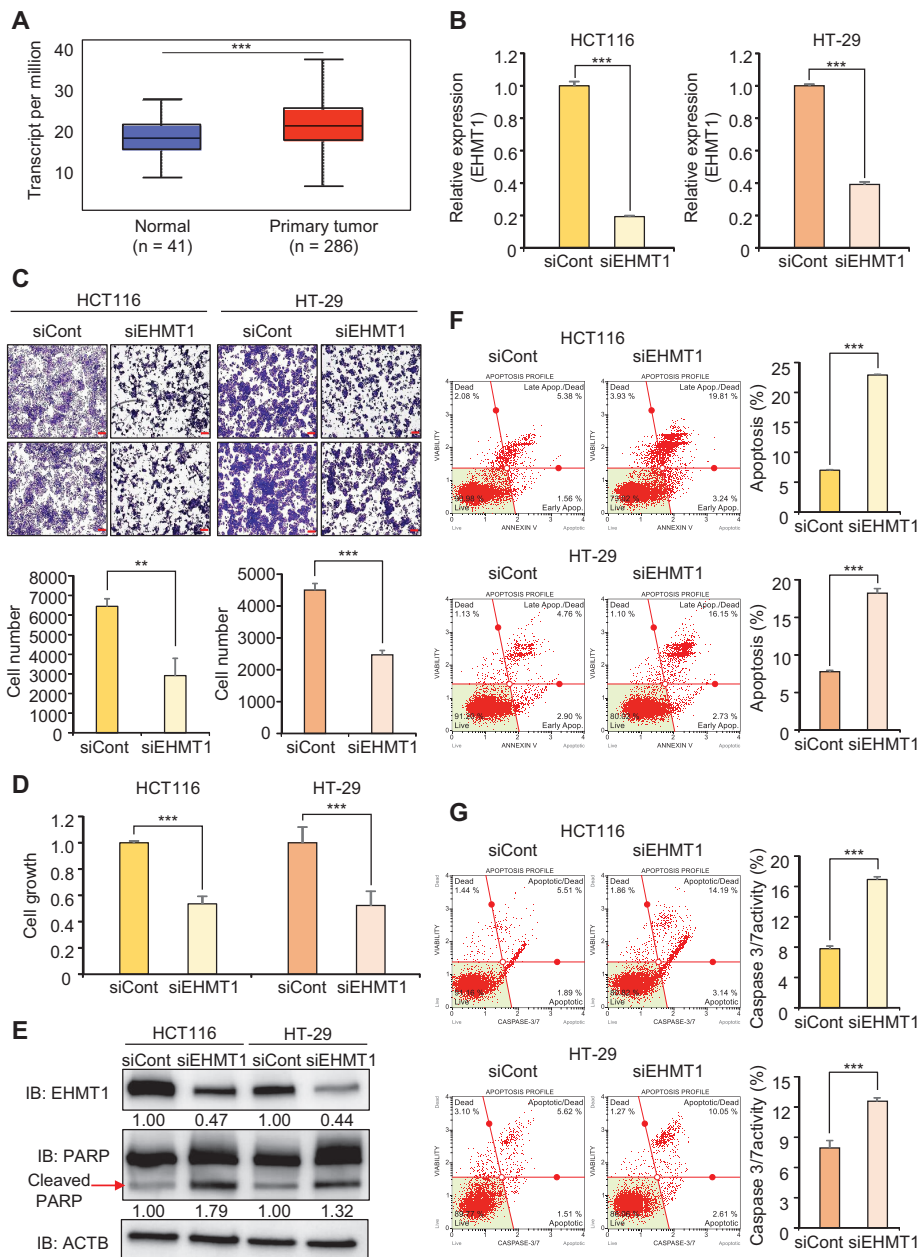
Fig. 1. Growth inhibition by EHMT1 knockdown in HCT116 and HT-29 cell lines. (A) Box plot of EHMT1 expression in CRC samples and normal samples from TCGA (http://ualcan.path.uab.edu/index.html). *P* values were calculated using Student's *t*-test (***$P < 0.001$). (B) qRT-PCR analysis of EHMT1 expression after transfection of siEHMT1 and siCont (negative control) into HCT116 (left) and HT-29 (right) cell lines. *P* values were calculated using Student's *t*-test (***$P < 0.001$). (C) Cell growth assay after transfection of siEHMT1 and siCont for 48 h. HCT116 and HT-29 cells were fixed in 100% methanol and stained with crystal violet solution. Scale bars = 200 μm (upper). The quantification of cell numbers. *P* values were calculated using Student's *t*-test (**$P < 0.01$, ***$P < 0.001$) (lower). (D) Cell viability assay after transfection of siEHMT1 and siCont for 48 h. HCT116 (left) and HT-29 (right) cells were incubated for 5 min at 37°C after addition of CCK-8 solution. The intensity of cell viability was measured using a microplate reader (450 nm). The mean ± SD of three independent experiments is shown. *P* values were calculated using Student's *t*-test (***$P < 0.001$). (E) Western blot analysis after EHMT1 knockdown using anti-EHMT1 and anti-PARP antibodies. ACTB was used as the internal control in HCT116 and HT-29 cells. The signal intensities were quantified using ImageJ software. IB, immunoblot. (F) FACS analysis using Muse annexin V staining was performed after EHMT1 knockdown. The lower right and upper right quadrants indicate early apoptosis and late apoptosis, respectively (left). Quantification of annexin V staining. The mean ± SD of three independent experiments is shown. *P* values were calculated using Student's *t*-test (***$P < 0.001$) (right). (G) FACS analysis using Muse Caspase-3/7 working solution was performed after EHMT1 knockdown. The upper right panel indicates the apoptotic and dead cell proportions (left). Quantification of caspase-3/7 activity is shown. The mean ± SD of three independent experiments is shown. *P* values were calculated using Student's *t*-test (***$P < 0.001$) (right).
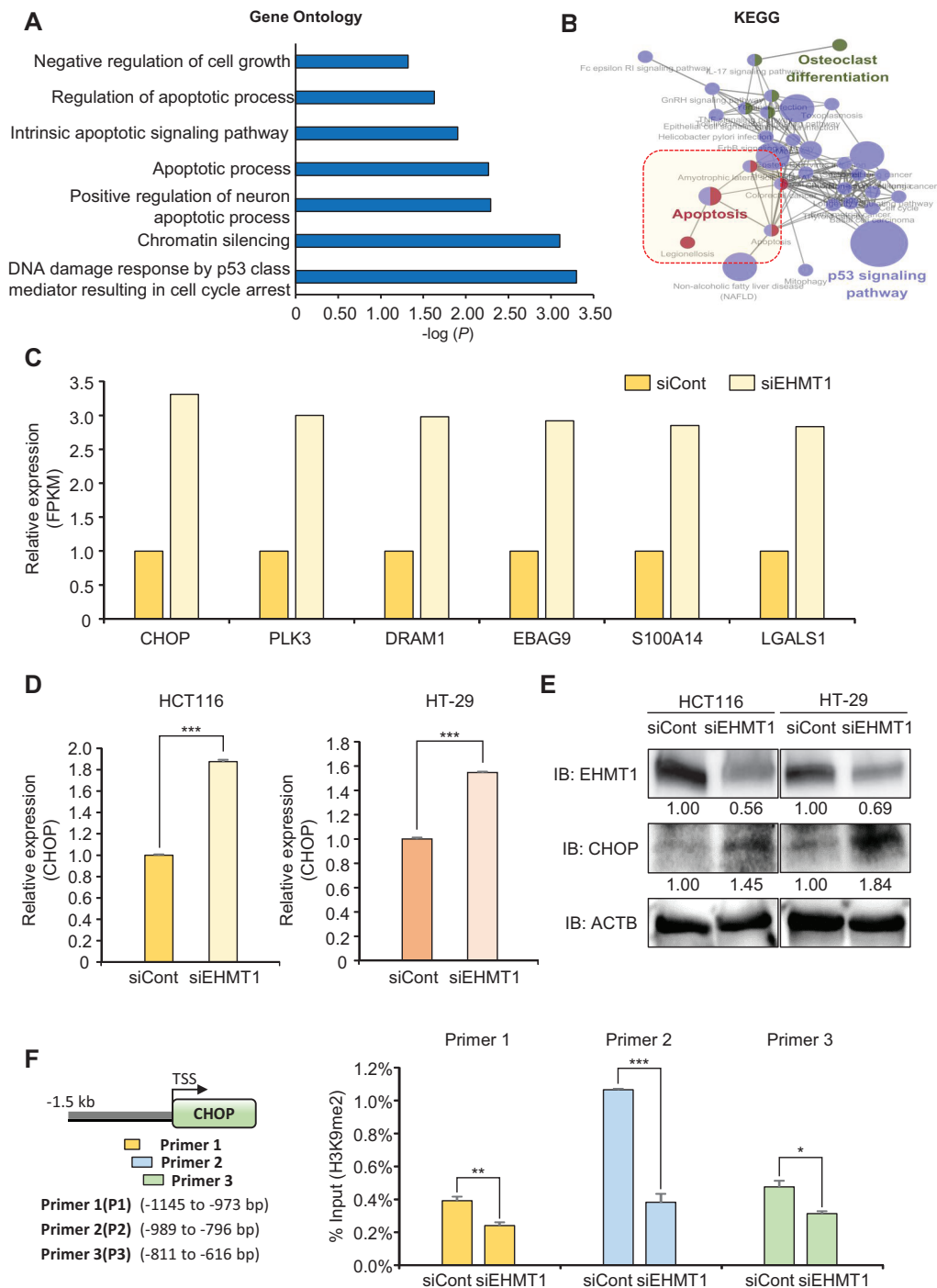
Fig. 2. Direct regulation of CHOP expression by EHMT1. (A) DAVID-based GO analysis of the upregulated genes among the 930 DEGs in the RNA-seq results. (B) GO pathway term enrichment networks. GO pathway term networks in the EHMT1 knockdown and control groups were functionally grouped by ClueGO. The cutoff value was set at $P > 0.05$. (C) Expression levels of *CHOP, PLK3, DRAM1, EBAG9, S100A14,* and *LGALS1* in the RNA-seq results after transfection of siEHMT1. (D) qRT-PCR analysis of CHOP expression after transfection of siEHMT1 into HCT116 (left) and HT-29 (right) cell lines. The mean ± SD of three independent experiments is shown. *P* values were calculated using Student's *t*-test (***P < 0.001). (E) Western blotting analysis after EHMT1 knockdown using anti-EHMT1 and anti-CHOP antibodies. ACTB was used as the internal control in HCT116 and HT-29 cells. The signal intensities were quantified using ImageJ software. IB, immunoblot. (F) Graphical abstract of design of ChIP primers specific for the CHOP promoter region (left). The ChIP assay was performed using an anti-H3K9me2 antibody. The results are expressed as a percentage of input chromatin compared with the control in HCT116 cells after siEHMT1 treatment. The mean ± SD of three independent experiments is shown. *P* values were calculated using Student's *t*-test (*P < 0.05, **P < 0.01, ***P < 0.001) (right).

were increased more than threefold in siEHMT1-treated cells compared to siCont-treated cells (Fig. 2C). CHOP, also known as DNA damage-inducible transcript 3 (DDIT3), is a proapoptotic transcription factor induced by endoplasmic reticulum (ER) stress. CHOP-induced apoptosis has been reported in several types of cancers, including breast cancer, pancreatic cancer and lung cancer (Hsin et al., 2012; Lin et al., 2013; Sanchez-Lopez et al., 2013). Expression of miR-211, a direct target of CHOP, induced by ER stress inhibits apoptosis by blocking CHOP accumulation (Chitnis et al., 2012). To confirm the CHOP overexpression seen in the RNA-seq results, we performed qPCR and western blotting after treatment with siEHMT1 and siCont. The expression of CHOP was increased by EHMT1 knockdown in HCT116 and HT-29 cells at the RNA and protein levels (Figs. 2D and 2E). Finally, we performed a ChIP assay to determine whether EHMT1 directly regulates CHOP. We designed three ChIP primers to target the promoter region of CHOP and performed a ChIP assay using an anti-H3K9me2 antibody (Fig. 2F, left). The H3K9me2 status was significantly decreased in the promoter region of CHOP by EHMT1 knockdown compared to that seen in the siCont group (Fig. 2F, right). Thus, these results suggest that EHMT1 directly regulates CHOP gene expression to prevent apoptosis of CRC cells.

Upregulation of CHOP expression by EHMT1 knockdown induces cell apoptosis in CRC

To determine whether upregulation of CHOP expression by EHMT1 knockdown induces cell apoptosis in CRC, we performed a cell growth assay after cotreatment of cells with siEHMT1 and siCHOP. qRT-PCR analysis showed that the expression of EHMT1 and CHOP was significantly decreased by siEHMT1 and siCHOP treatment, and we reconfirmed the upregulation of CHOP expression by EHMT1 knockdown only (Fig. 3A). In the cell growth assay with CV staining and CCK-8 analysis, the reduction in cell growth induced by EHMT1 knockdown was recovered after cotransfection with siEHMT1 and siCHOP (Figs. 3B and 3C). In addition, western blotting analysis showed that the induction of cleaved PARP by EHMT1 knockdown was decreased by CHOP downregulation (Fig. 3D). Moreover, in the FACS analysis, we confirmed that caspase 3/7 activity was decreased by cotransfection with siEHMT1 and siCHOP (Fig. 3E). Thus, CHOP regulation by EHMT1 knockdown likely induces cell apoptosis to inhibit the growth of CRC cell lines.

DISCUSSION

Epigenetic modifications such as histone modification, DNA methylation, miRNA modification, and noncoding RNA modification play an important role by regulating genes in tumor development. In particular, epigenetic machinery regulates CRC development processes, such as growth, metastasis, and drug resistance. Wang et al. (2021) reported that downregulation of WHSC1, a histone methyltransferase inducing H3K36 methylation, promotes chemosensitivity to oxaliplatin and 5-fluorouracil in CRC (Baretti and Azad, 2018; Han et al., 2020; Huang et al., 2017; Ryu et al., 2019; Wang et al., 2021). Therefore, novel anticancer inhibitors targeting

epigenetic modifications can be used directly or may have a synergistic effect with well-known anticancer drugs.

In this study, CHOP was selected as a target of EHMT1; CHOP is a well-known ER stress-related gene. ER stress induces the unfolded protein response, causing the well-regulated activation of intracellular signaling responses designed to restore protein homeostasis. ER stress-mediated apoptosis occurs via the PERK/elF2a/ATF4/CHOP axis and suppresses tumor development in several types of cancer (Carracedo et al., 2006; Guha et al., 2017; Hwang et al., 2020; Park et al., 2007; 2010; Rozpedek et al., 2016; Zhang et al., 2018). Here, we identified that EHMT1 directly regulates CHOP expression by controlling H3K9 methylation in the CHOP promoter region (Fig. 2). Moreover, we identified that the EHMT1-related cell apoptosis induced by CHOP regulation in CRC may be an ER stress-independent process because the expression levels of GRP78 and ATF4, which are ER stress markers, were not upregulated by EHMT1 knockdown in HCT116 and HT-29 cell lines (Supplementary Fig. S1). Thus, the EHMT1-CHOP axis regulating cell apoptosis may be an important factor for CRC development.

EHMT1 and EHMT2 have 80% homology in the SET domain and form a heterodimer to perform H3K9 monomethylation and dimethylation. In addition, EHMT1/2 interacts with ZNF644 to catalyze the conversion of adenosyl-L-methionine molecules into H3K9me1/2 (Herz et al., 2013; Olsen et al., 2016). Hwang et al. (2020) reported that BIX-01294, an inhibitor of EHMT2, induced cell apoptosis via upregulation of CHOP and Ras-related GTP binding C (RRAGC) expression in liver cancer cell lines. In RNA-seq and qRT-PCR analyses after EHMT2 knockdown in HCT116 cell lines, we also found upregulation of CHOP expression by EHMT2 knockdown, in addition to CHOP induction by EHMT1 knockdown (Supplementary Fig. S2). Overall, we hypothesized that (1) CHOP may also be a direct target of EHMT2 and (2) the complex of EHMT1 and EHMT2 may directly regulate CHOP expression to control the apoptosis process in CRC.

In a previous study, we reported that EHMT1 regulates CDKN1A gene expression through epigenetic regulation and consequently plays a critical role in the regulation of lung cancer cell apoptosis and the cell cycle (Lee et al., 2021). Therefore, we expected that EHMT1 would affect cell cycle regulation in colon cancer. The RNA-seq results of EHMT1-knockdown cells showed that the expression of cell cycle-related genes (Ausserlechner et al., 2004; Kim et al., 2019; 2020; Wang et al., 2009; 2020; Yuan et al., 2015) (CCNA2, CCNB1, CCNB2, CCND3, CCNE1, CCNE2, CDK6, E2F1, E2F2, and E2F7) was significantly downregulated and that CDKN1A expression was also upregulated by EHMT1 knockdown (Supplementary Fig. S3). Thus, although we suggest that apoptosis-related EHMT1 functions by regulating CHOP expression in this study, we also suggest that EHMT1 is an important regulator of the cell cycle and apoptosis, thus affecting colon cancer proliferation, and that the CHOP-related apoptosis induced by EHMT1 knockdown is an EHMT1-related apoptosis pathway.

In conclusion, the expression of EHMT1 was increased in CRC samples compared to normal samples. We observed that EHMT1 knockdown inhibited the growth of CRC cell
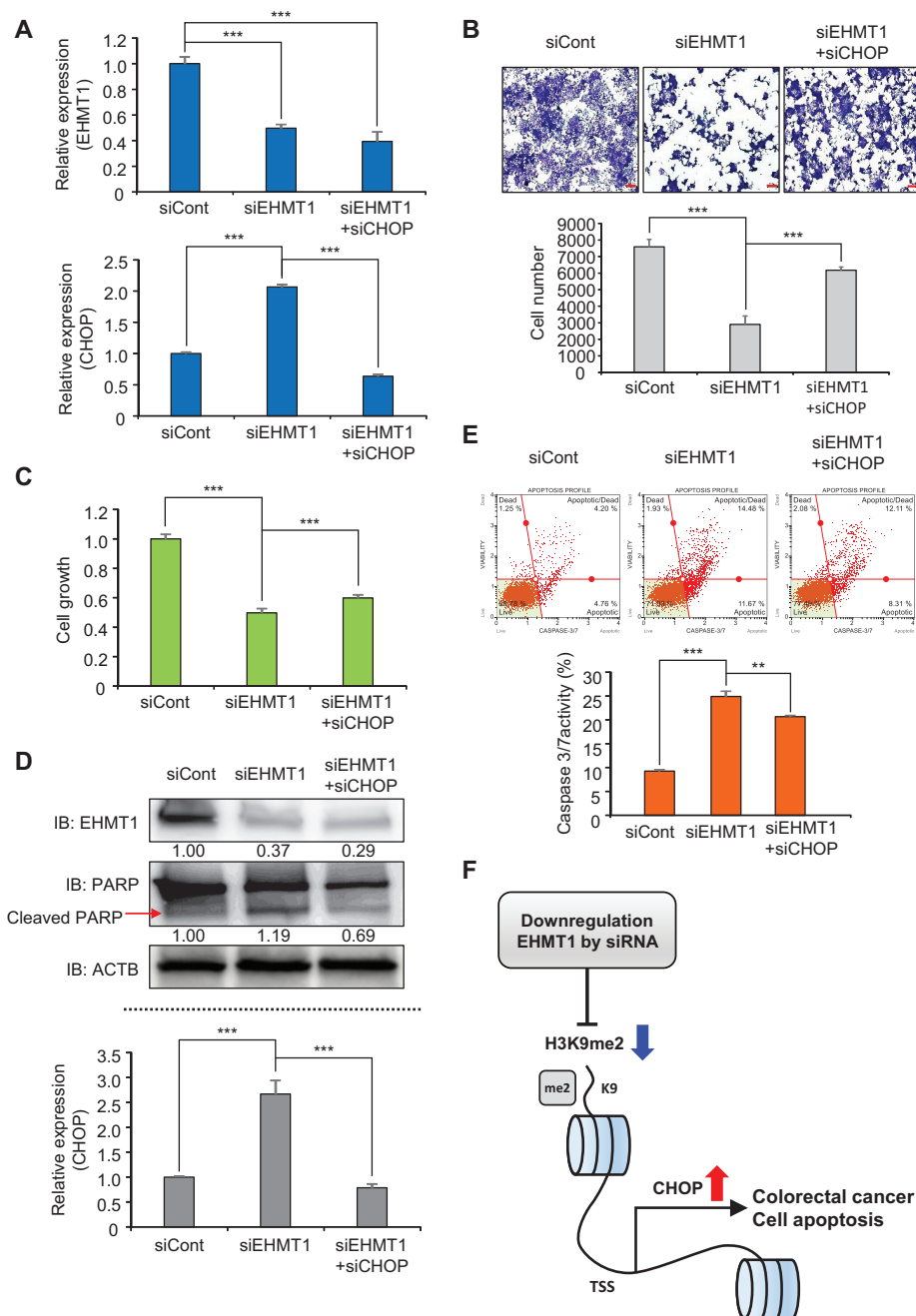
Fig. 3. Induction of apoptosis by EHMT1 knockdown related CHOP up-regulation. (A) qRT-PCR analysis of EHMT1 (upper) and CHOP (lower) expression after cotransfection of siEHMT1 and siCHOP into HCT116 cells. The mean ± SD of three independent experiments is shown. *P* values were calculated using Student's *t*-test (***P < 0.001). (B) Cell growth assay after cotransfection of siEHMT1 and siCHOP for 48 h. HCT116 cells were fixed in 100% methanol and stained with crystal violet solution. Scale bars = 200 μm (upper). The quantification of cell numbers. *P* values were calculated using Student's *t*-test (***P < 0.001) (lower). (C) Cell viability assay after cotransfection of siEHMT1 and siCHOP for 48 h. HCT116 cells were incubated for 5 min at 37°C after addition of CCK-8 solution. The intensity of cell viability was measured using a microplate reader (450 nm). The mean ± SD of three independent experiments is shown. *P* values were calculated using Student's *t*-test (***P < 0.001). (D) Western blotting analysis (upper) after cotransfection of siEHMT1 and siCHOP using anti-EHMT1 and anti-PARP antibodies. ACTB was used as the internal control in HCT116 cells. The signal intensities were quantified using ImageJ software. qRT-PCR analysis (lower) of CHOP after cotransfection of siEHMT1 and siCHOP in HCT116 cells. The mean ± SD of three independent experiments is shown. *P* values were calculated using Student's *t*-test (***P < 0.001). IB, immunoblot. (E) FACS analysis using Muse Caspase-3/7 working solution was performed after cotransfection of siEHMT1 and siCHOP. The upper right panel indicates the apoptotic and dead cell proportions (upper). Quantification of caspase-3/7 activity is shown. The mean ± SD of three independent experiments is shown. *P* values were calculated using Student's *t*-test (**P < 0.01, ***P < 0.001) (lower). (F) Schematic summary of EHMT1 function in CRC.

lines by inducing apoptosis by upregulating the expression of CHOP, which was identified as a direct target of EHMT1 with a ChIP assay using anti-H3K9me2 antibodies. Finally, cotransfection of cells with siEHMT1 and siCHOP revealed that the apoptotic process induced by EHMT1 knockdown occurred via the regulation of CHOP expression (Fig. 3F). Therefore, we expect that EHMT1 could become a therapeutic target for the development of drugs to treat CRC.

Note: Supplementary information is available on the Molecules and Cells website (www.molcells.org).

ACKNOWLEDGMENTS

AUTHOR CONTRIBUTIONS

S.K.K. and H.-S.C. conceived and designed the study. K.K., T.Y.R., and J.L. developed the methodology. D.-S.K. analyzed and interpreted the data. K.K., M.-Y.S., D.-S.K., S.K.K., and H.-S.C. wrote and reviewed the manuscript. S.K.K. and H.-S. C. supervised the study.

CONFLICT OF INTEREST

The authors have no potential conflicts of interest to disclose.

ORCID

Kwangho Kim   https://orcid.org/0000-0001-9387-7642
Tae Young Ryu   https://orcid.org/0000-0001-8429-383X
Jinkwon Lee   https://orcid.org/0000-0002-7416-6359
Mi-Young Son   https://orcid.org/0000-0001-7590-8812
Dae-Soo Kim   https://orcid.org/0000-0002-4999-1613
Sang Kyum Kim   https://orcid.org/0000-0001-5769-0792
Hyun-Soo Cho   https://orcid.org/0000-0002-8242-9390

REFERENCES

Ausserlechner, M.J., Obexer, P., Bock, G., Geley, S., and Kofler, R. (2004). Cyclin D3 and c-MYC control glucocorticoid-induced cell cycle arrest but not apoptosis in lymphoblastic leukemia cells. Cell Death Differ. *11*, 165-174.

Baretti, M. and Azad, N.S. (2018). The role of epigenetic therapies in colorectal cancer. Curr. Probl. Cancer *42*, 530-547.

Carracedo, A., Gironella, M., Lorente, M., Garcia, S., Guzman, M., Velasco, G., and Iovanna, J.L. (2006). Cannabinoids induce apoptosis of pancreatic tumor cells via endoplasmic reticulum stress-related genes. Cancer Res. *66*, 6748-6755.

Cebrian, A., Pharoah, P.D., Ahmed, S., Ropero, S., Fraga, M.F., Smith, P.L., Conroy, D., Luben, R., Perkins, B., Easton, D.F., et al. (2006). Genetic variants in epigenetic genes and breast cancer risk. Carcinogenesis *27*, 1661-1669.

Chitnis, N.S., Pytel, D., Bobrovnikova-Marjon, E., Pant, D., Zheng, H., Maas, N.L., Frederick, B., Kushner, J.A., Chodosh, L.A., Koumenis, C., et al. (2012). miR-211 is a prosurvival microRNA that regulates chop expression in a PERK-dependent manner. Mol. Cell *48*, 353-364.

Ea, C.K., Hao, S., Yeo, K.S., and Baltimore, D. (2012). EHMT1 protein binds to nuclear factor-κB p50 and represses gene expression. J. Biol. Chem. *287*, 31207-31217.

Guan, X., Zhong, X., Men, W., Gong, S., Zhang, L., and Han, Y. (2014). Analysis of EHMT1 expression and its correlations with clinical significance in esophageal squamous cell cancer. Mol. Clin. Oncol. *2*, 76-80.

Guha, P., Kaptan, E., Gade, P., Kalvakolanu, D.V., and Ahmed, H. (2017). Tunicamycin induced endoplasmic reticulum stress promotes apoptosis of prostate cancer cells by activating mTORC1. Oncotarget *8*, 68191-68207.

Han, X., Luan, T., Sun, Y., Yan, W., Wang, D., and Zeng, X. (2020). MicroRNA 449c mediates the generation of monocytic myeloid-derived suppressor cells by targeting STAT6. Mol. Cells *43*, 793-803.

Herz, H.M., Garruss, A., and Shilatifard, A. (2013). SET for life: biochemical activities and biological functions of SET domain-containing proteins. Trends Biochem. Sci. *38*, 621-639.

Hsin, I.L., Hsiao, Y.C., Wu, M.F., Jan, M.S., Tang, S.C., Lin, Y.W., Hsu, C.P., and Ko, J.L. (2012). Lipocalin 2, a new GADD153 target gene, as an apoptosis inducer of endoplasmic reticulum stress in lung cancer cells. Toxicol. Appl. Pharmacol. *263*, 330-337.

Huang, T., Lin, C., Zhong, L.L., Zhao, L., Zhang, G., Lu, A., Wu, J., and Bian, Z. (2017). Targeting histone methylation for colorectal cancer. Therap. Adv. Gastroenterol. *10*, 114-131.

Hwang, S., Kim, S., Kim, K., Yeom, J., Park, S., and Kim, I. (2020). Euchromatin histone methyltransferase II (EHMT2) regulates the expression of ras-related GTP binding C (RRAGC) protein. BMB Rep. *53*, 576-581.

Jung, G., Hernandez-Illan, E., Moreira, L., Balaguer, F., and Goel, A. (2020). Epigenetics of colorectal cancer: biomarker and therapeutic potential. Nat. Rev. Gastroenterol. Hepatol. *17*, 111-130.

Kim, K., Kwon, O., Ryu, T.Y., Jung, C.R., Kim, J., Min, J.K., Kim, D.S., Son, M.Y., and Cho, H.S. (2019). Propionate of a microbiota metabolite induces cell apoptosis and cell cycle arrest in lung cancer. Mol. Med. Rep. *20*, 1569-1574.

Kim, S., Kim, J., Jung, Y., Jun, Y., Jung, Y., Lee, H.Y., Keum, J., Park, B.J., Lee, J., Kim, J., et al. (2020). Characterization of TNNC1 as a novel tumor suppressor of lung adenocarcinoma. Mol. Cells *43*, 619-631.

Kleefstra, T., Kramer, J.M., Neveling, K., Willemsen, M.H., Koemans, T.S., Vissers, L.E., Wissink-Lindhout, W., Fenckova, M., van den Akker, W.M., Kasri, N.N., et al. (2012). Disruption of an EHMT1-associated chromatin-modification module causes intellectual disability. Am. J. Hum. Genet. *91*, 73-82.

Koopman, M., Antonini, N.F., Douma, J., Wals, J., Honkoop, A.H., Erdkamp, F.L., de Jong, R.S., Rodenburg, C.J., Vreugdenhil, G., Loosveld, O.J., et al. (2007). Sequential versus combination chemotherapy with capecitabine, irinotecan, and oxaliplatin in advanced colorectal cancer (CAIRO): a phase III randomised controlled trial. Lancet *370*, 135-142.

Kuipers, E.J., Grady, W.M., Lieberman, D., Seufferlein, T., Sung, J.J., Boelens, P.G., van de Velde, C.J., and Watanabe, T. (2015). Colorectal cancer. Nat. Rev. Dis. Primers *1*, 15065.

Lee, J., Kim, K., Ryu, T.Y., Jung, C.R., Lee, M.S., Lim, J.H., Park, K., Kim, D.S., Son, M.Y., Hamamoto, R., et al. (2021). EHMT1 knockdown induces apoptosis and cell cycle arrest in lung cancer cells by increasing CDKN1A expression. Mol. Oncol. *15*, 2989-3002.

Lin, S., Zhang, J., Chen, H., Chen, K., Lai, F., Luo, J., Wang, Z., Bu, H., Zhang, R., Li, H., et al. (2013). Involvement of endoplasmic reticulum stress in capsaicin-induced apoptosis of human pancreatic cancer cells. Evid. Based

Complement. Alternat. Med. *2013*, 629750.

Ohno, H., Shinoda, K., Ohyama, K., Sharp, L.Z., and Kajimura, S. (2013). EHMT1 controls brown adipose cell fate and thermogenesis through the PRDM16 complex. Nature *504*, 163-167.

Olsen, J.B., Wong, L., Deimling, S., Miles, A., Guo, H., Li, Y., Zhang, Z., Greenblatt, J.F., Emili, A., and Tropepe, V. (2016). G9a and ZNF644 physically associate to suppress progenitor gene expression during neurogenesis. Stem Cell Reports *7*, 454-470.

Park, J.W., Woo, K.J., Lee, J.T., Lim, J.H., Lee, T.J., Kim, S.H., Choi, Y.H., and Kwon, T.K. (2007). Resveratrol induces pro-apoptotic endoplasmic reticulum stress in human colon cancer cells. Oncol. Rep. *18*, 1269-1273.

Park, S.K., Sanders, B.G., and Kline, K. (2010). Tocotrienols induce apoptosis in breast cancer cell lines via an endoplasmic reticulum stress-dependent increase in extrinsic death receptor signaling. Breast Cancer Res. Treat. *124*, 361-375.

Renneville, A., Van Galen, P., Canver, M.C., McConkey, M., Krill-Burger, J.M., Dorfman, D.M., Holson, E.B., Bernstein, B.E., Orkin, S.H., Bauer, D.E., et al. (2015). EHMT1 and EHMT2 inhibition induces fetal hemoglobin expression. Blood *126*, 1930-1939.

Rozpedek, W., Pytel, D., Mucha, B., Leszczynska, H., Diehl, J.A., and Majsterek, I. (2016). The role of the PERK/eIF2α/ATF4/CHOP signaling pathway in tumor progression during endoplasmic reticulum stress. Curr. Mol. Med. *16*, 533-544.

Ryu, T.Y., Kim, K., Son, M.Y., Min, J.K., Kim, J., Han, T.S., Kim, D.S., and Cho, H.S. (2019). Downregulation of PRMT1, a histone arginine methyltransferase, by sodium propionate induces cell apoptosis in colon cancer. Oncol. Rep. *41*, 1691-1699.

Sanchez-Lopez, E., Zimmerman, T., Gomez del Pulgar, T., Moyer, M.P., Lacal Sanjuan, J.C., and Cebrian, A. (2013). Choline kinase inhibition induces exacerbated endoplasmic reticulum stress and triggers apoptosis via CHOP in cancer cells. Cell Death Dis. *4*, e933.

Sung, H., Ferlay, J., Siegel, R.L., Laversanne, M., Soerjomataram, I., Jemal, A., and Bray, F. (2021). Global cancer statistics 2020: GLOBOCAN estimates of incidence and mortality worldwide for 36 cancers in 185 countries. CA Cancer J. Clin. *71*, 209-249.

Thienpont, B., Aronsen, J.M., Robinson, E.L., Okkenhaug, H., Loche, E., Ferrini, A., Brien, P., Alkass, K., Tomasso, A., Agrawal, A., et al. (2017). The H3K9 dimethyltransferases EHMT1/2 protect against pathological cardiac hypertrophy. J. Clin. Invest. *127*, 335-348.

Wang, F., Fu, X.D., Zhou, Y., and Zhang, Y. (2009). Down-regulation of the cyclin E1 oncogene expression by microRNA-16-1 induces cell cycle arrest in human cancer cells. BMB Rep. *42*, 725-730.

Wang, Y., Pei, X., Xu, P., Tan, Z., Zhu, Z., Zhang, G., Jiang, Z., and Deng, Z. (2020). E2F7, regulated by miR30c, inhibits apoptosis and promotes cell cycle of prostate cancer cells. Oncol. Rep. *44*, 849-862.

Wang, Y., Zhu, L., Guo, M., Sun, G., Zhou, K., Pang, W., Cao, D., Tang, X., and Meng, X. (2021). Histone methyltransferase WHSC1 inhibits colorectal cancer cell apoptosis via targeting anti-apoptotic BCL2. Cell Death Discov. *7*, 19.

Xie, Y.H., Chen, Y.X., and Fang, J.Y. (2020). Comprehensive review of targeted therapy for colorectal cancer. Signal Transduct. Target. Ther. *5*, 22.

Yang, Y., Shen, J., Yan, D., Yuan, B., Zhang, S., Wei, J., and Du, T. (2018). Euchromatic histone lysine methyltransferase 1 regulates cancer development in human gastric cancer by regulating E-cadherin. Oncol. Lett. *15*, 9480-9486.

Yuan, L., Zhang, Y., Xia, J., Liu, B., Zhang, Q., Liu, J., Luo, L., Peng, Z., Song, Z., and Zhu, R. (2015). Resveratrol induces cell cycle arrest via a p53-independent pathway in A549 cells. Mol. Med. Rep. *11*, 2459-2464.

Zhang, M., Du, H., Huang, Z., Zhang, P., Yue, Y., Wang, W., Liu, W., Zeng, J., Ma, J., Chen, G., et al. (2018). Thymoquinone induces apoptosis in bladder cancer cell via endoplasmic reticulum stress-dependent mitochondrial pathway. Chem. Biol. Interact. *292*, 65-75.